Pergamon

SCIENCE DIRECT®

Tetrahedron 59 (2003) 1981–1988

TETRAHEDRON

# Proton NMR study on two structures of 3′-*O*-(acetylimino)3′-de(phosphinico)-thymidylyl-(3,5′)-deoxythymidine in aqueous solution

Yu-Yu Tseng,[a] Te-Fang Yang[b] and Lou-sing Kan[a,*]

[a]*Institute of Chemistry, Academia Sinica, Nankang, Taipei 11529, Taiwan, ROC*
[b]*Department of Applied Chemistry, Chaoyang University of Technology, Wufeng, Taichung 413, Taiwan, ROC*

Received 18 November 2002; accepted 20 January 2003

**Abstract**—The solution structure of one of dithymidine monophosphate (TpT) analogues, containing an (*N*-acetyl)imino backbone linkage ($NCOCH_3$) of 3′-*O*-(acetylimino)3′-de(phosphinico)-thymidylyl-(3,5′)-deoxythymidine ($T_NT$), has been determined by proton NMR. Two structures, designated as major and minor forms, in a ratio of about 3:2 coexist when the solution temperature is <25°C. Both forms adopt *anti* conformation with respect to the glycosidic bond, S-type deoxyribofuranose pucker, and have no base stacking. The backbone torsion angles $\varepsilon'$, $\phi_{ON}$, $\phi_{NC}$, and $\gamma'$ are *trans*, *gauche* $^+$, *gauche* $^+$, and *gauche* $^+$ for the major form; and *gauche* $^-$, *gauche* $^-$, *gauche* $^-$, and *gauche* $^+$ for the minor form. Only major form is found at >25°C. 

## 1. Introduction

A search for promising oligonucleotides as potential antisense agents has been pursued aggressively in the last decade.[1–5] The typical difference between the naturally occurring oligonucleotides and the synthetic antisense oligomers is that the phosphate linkage of the former is usually replaced by neutral functionality[6] as far as structural stability of the latter is concerned. Although most of the reported modified linkages contained in dinucleotides as part of a single strand are four-atom motifs (O–X–O–C), shown in Structure A, a few nucleoside dimers, in which the linkage is composed of a three-atom chain (O–X–C), shown in Structure B, have been synthesized and investigated.[6–8]

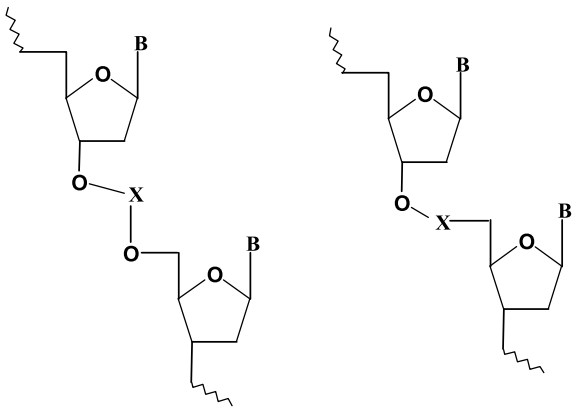


**Structure A** **Structure B**

For example, Richert and co-workers[8] reported that methyl sulfide and methyl sulfoxide linkage, a four-atom motif, could be incorporated into DNA oligomers, and sequence-specific binding was observed. On the other hand, Burgess et al.[6] reported that an oxyamide linked nucleotide dimer that contained a three-atom motif has been successfully incorporated into an oligodeoxynucleotide. It was found that the novel synthetic strand showed almost the same binding affinity as the natural one by forming duplexes with their DNA and RNA complements. Nevertheless, the optimal structure of modified backbone for stable binding has not been thoroughly studied or understood. In this paper, we focus our attention on the structural studies of dinucleoside with modified linkages. The dimeric deoxyribonucleoside under current study was a novel thymidine dimers with three-atom backbone that was a derivative of oxyamide in the backbones, 3′-*O*-(acetylimino)3′-de(phosphinico)-thymidylyl-(3,5′)-deoxythymidine ($T_NT$) (Fig. 1).[9] The structure of the aforementioned dimer was studied by proton NMR spectroscopy that has been widely applied to the study of biological molecules in aqueous solution.[10–12] We choose (*N*-acetyl)imino group as the backbone of novel dinucleotide because it is isosteric to oxyamide group.[6] A unique feature of $T_NT$ is that its NMR signals split into

*Keywords*: 3′-*O*-(acetylimino)3′-de(phosphinico)-thymidylyl-(3,5′)-deoxythymidine ($T_NT$); chemical shift; coupling constant; nuclear magnetic resonance (NMR); nuclear Overhauser enhancement (NOE); 2D COSY; 2D NOESY.

* Corresponding author. Tel.: +886-2-2789-8550; fax: +886-2-2783-1237; e-mail: lskan@chem.sinica.edu.tw

0040–4020/03/$ - see front matter 
doi:10.1016/S0040-4020(03)00141-8

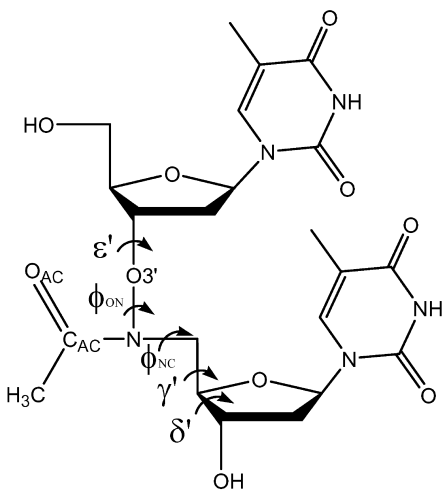


**Figure 1.** Compound $T_NT$. The (*N*-acetyl)imino linkage is defined in the figure. There are two atoms (O and N) between $C_{3'}$ of one nucleotide and $C_{5'}$ of the other instead of three (O, P, and O) in a normal nucleotide linkage. The $C_{3'}-O_{3'}$ and $C_{4'}-C_{5'}$ were named traditional. The dihedral angles between $O_{3'}-N$ and $N-C_{5'}$ are defined as $\phi_{ON}$ and $\phi_{NC}$, respectively.

two sets at temperatures lower than 25°C. This result indicates that two stable structures of $T_NT$ co-exists in aqueous solution—a phenomenon has never been observed in either dithymidine monophosphates[13] or in any other natural dinucleoside monophosphates.[14] These two $T_NT$ structures were determined by NMR data, including chemical shifts, coupling constants, and NOE's.

## 2. Results

### 2.1. The assignment of proton resonance of $T_NT$ at high and low temperatures

The pattern of proton NMR spectrum of $T_NT$ in $D_2O$ is well resolved at 35°C and above (Fig. 2). Thus, the assignment of all proton resonance in $D_2O$ was determined by the recognition that $H_{5'}$ and $H_{5''}$ of $_NT$ are more downfield than those in $T_N$. Thus, their identities can be recognized by chemical shift values, coupling patterns, and 2D COSY spectrum (data not shown). In turn, the assignments of $H_{4'}$, $H_{3'}$, $H_{2'}$, $H_{2''}$, and $H_{1'}$ on the sugar moiety of $T_N$ and $_NT$, respectively, can also be sequentially assigned by 2D COSY (data not shown). The identity of $C_6-H$ was determined by assigning cross peaks with $H_{1'}$ by 2D NOESY (data not shown). $C_5-CH_3$ was then determined by its cross peak with $C_6-H$. The methyl group of $NCOCH_3$ ($COCH_3$) can be readily assigned by its resonance pattern (singlet) and intensity (three protons). The assignments at high temperature (>35°C) coincide with those reported previously in DMSO-$d_6$.[9] However, it is interesting to note that all proton resonance of $T_NT$, as well as the $COCH_3$ signal split into two sets with a chemical shift difference from <0.01 to 0.10 ppm when the temperature was lower than 25°C (Figs. 2–4 and Table 1). For instance, the $C_6-H$ peak of $_NT$, (at 7.3 ppm, indicated by ↓ in Fig. 2), became broader as the temperature was lowered to 25°C, then a shoulder appeared at 15°C, and finally two peaks can be resolved at 10°C (Figs. 2 and 3). These two peaks became sharper as the temperature was lowered further (Fig. 3). These results suggested that $T_NT$ has two structures co-existing in low

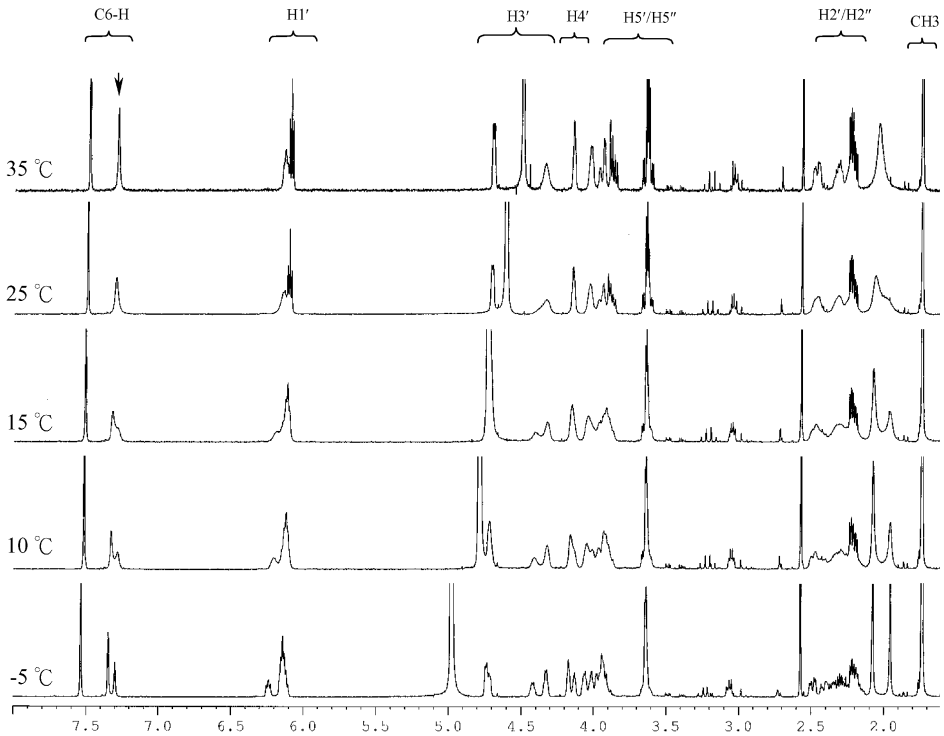


**Figure 2.** 1D spectra of $T_NT$ at a few selected temperatures. The chemical shift is referenced to DSS. The identities of base, sugar, and COCH3 signals are denoted at top of the figure. The detail chemical shift values are collected in Table 1. The ↓ singles out the splitting peak as temperature lowered (see below). There are traces of impurities in chemical range of 3.0–3.3 ppm.

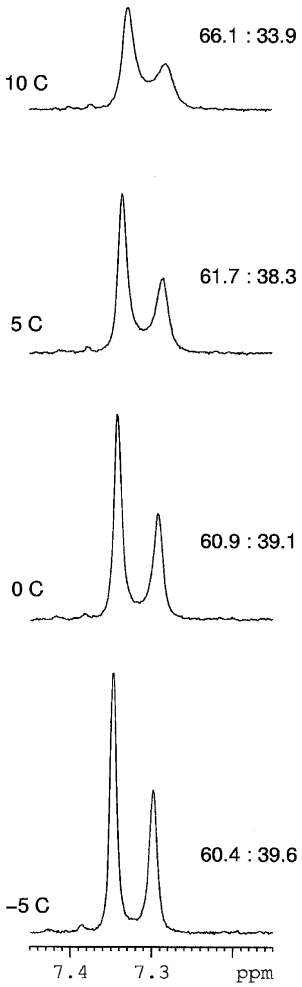


**Figure 3.** Temperature-dependent ratios of major and minor $C_6$–H peaks areas of $_N$T moiety in $T_NT$.

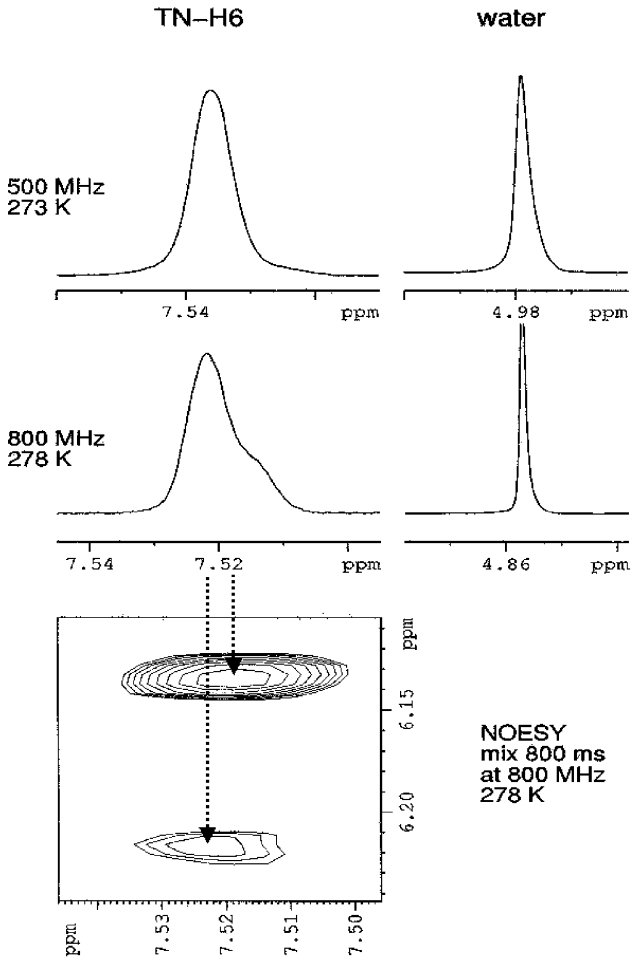


**Figure 4.** The signal of $C_6$–H of $T_N$– was a singlet at 500 MHz but showed a shoulder compared to the line shape of HDO peak of solvent at 800 MHz at 5°C.

temperatures. Some of the splits are too small to be observed by 500 MHz but are seen at 800 MHz at 5°C (Table 1 and Fig. 4). As shown in Figure 4, the signal of $C_6$–H of $T_N$- was a singlet at 500 MHz but showed a shoulder compared to the line shape of HDO peak of solvent at 800 MHz at 5°C. However, the newly formed peaks are less in intensity and we called this new conformer 'minor', whereas the more abundant form 'major'. The major form has the same structure as $T_NT$ at high temperatures, traced by the same chemical shift values of all resonance of $T_N$, $_N$T, and $COCH_3$ moieties (Table 1). The assignment of the minor form can be determined by 2D COSY and 2D NOESY. For instance, the C6-H of the minor form at 7.52 ppm has an NOE with a peak at 6.13 ppm identifiable as the $H_{1'}$ (Fig. 4). The rest of the signals of minor form can be assigned by 2D COSY (data not shown) and the results are summarized in Table 1.

The ratio of these two forms can be estimated by integrating the areas under the well split signals (i.e. $C_6$–H of $_N$T). As shown in Figure 3, the ratios are 66:34, 62:38, 61:39, and 60:40 at 10, 5, 0, and −5°C, respectively. Thus, these two structures reach an equilibrium at a ratio about 3:2. Similar results can be obtained when $COCH_3$ is accounted for at low temperatures (data not shown).

## 2.2. The study of the structure of $T_NT$ at high temperatures and the major form at low temperatures

There are 14 inter-nucleoside NOE connections identifiable at 55°C (Fig. 5(a) and (b)). Comparing to the NOE intensities between $H_{2'}$ and $H_{2''}$, five of them have medium intensities and the rest are weak (Fig. 5(a)). Totally, six NOE's (one of them is medium and five of them are weak) are originated by the inter-nucleoside proton pairs. Those effects are of $H_{1'}$ ($T_N$) to $H_{5'}$ ($_N$T) (weak), $H_{3'}$ ($T_N$) to $H_{4'}$ ($_N$T) (weak), $H_6$ ($_N$T) to $H_{2'}$ (medium), $H_{3'}$ (weak), and $H_{4'}$ (weak) ($T_N$), and $C_5$–$CH_3$ ($_N$T) to $H_{1'}$ ($T_N$) (weak). The $COCH_3$ was related to the rest of observed NOE's. Namely, the $COCH_3$ has NOE to $H_{1'}$ (medium), $H_{2'}$ (medium), $H_{3'}$ (weak), and $H_{4'}$ (weak) of $T_N$ and to $C_6$–H (weak), $H_{4'}$ (weak), $H_{5'}$ (medium), and $H_{5''}$ (medium) of $_N$T, respectively (Fig. 5(a) and (b)). This result might indicate that the $CH_3$ group of $-COCH_3$ is close to both $T_N$ and $_N$T moieties at 55°C. These NOE data were used for DG and MD calculations as described in Materials and Methods. The resultant structure shown in Figure 6(A) has the lowest energy and is also consistent with all the NMR data observed. As shown in Figure 6(A), the two thymine bases of $T_NT$ stretch out (Fig. 6(A)(1)) and are nearly perpendicular to each other (Fig. 6(A)(2)), ensuring least

**Table 1**. Temperature dependent chemical shifts (ppm) of $T_NT$

| $T_N$ | H6 | C5–$CH_3$ | H1′ | H2′ | H2″ | H3′ | H4′ | H5′, H5″ |
|---|---|---|---|---|---|---|---|---|
| 35°C | 7.48 | 1.74 | 6.13 | 2.47 | 2.21 | 4.69 | 4.14 | 3.63 |
| 25°C | 7.50 | 1.74 | 6.14 | 2.47 | 2.21 | 4.70 | 4.15 | 3.63 |
| 20°C | 7.50 | 1.74 | 6.14 | 2.46 | 2.21 | 4.71 | 4.15 | 3.63 |
| 15°C | 7.51 | 1.74 | 6.11/6.19 | 2.46 | 2.21 | 4.71 | 4.15 | 3.64 |
| 10°C | 7.51 | 1.73 | 6.12/6.21 | 2.49/2.41[a] | 2.27/2.17 | 4.71 | 4.16/4.14 | 3.64 |
| 5°C[b] | 7.53/7.51 | 1.73 | 6.13/6.22 | 2.49/2.41 | 2.27/2.17 | 4.73/4.71 | 4.17/4.13 | 3.64 |
| 0°C | 7.53 | 1.73 | 6.14/6.23 | 2.49/2.41 | 2.27/2.17 | 4.73/4.71 | 4.17/4.13 | 3.64 |

| $_NT$ | H6 | C5–$CH_3$ | H1′ | H2′ | H2″ | H3′ | H4′ | H5′, H5″ |
|---|---|---|---|---|---|---|---|---|
| 35°C | 7.29 | 1.74 | 6.09 | 2.24 | 2.32 | 4.34 | 4.02 | 3.87, 3.95 |
| 25°C | 7.30 | 1.74 | 6.10 | 2.24 | 2.32 | 4.33 | 4.03 | 3.88, 3.96 |
| 20°C | 7.31 | 1.74 | 6.11 | 2.23 | 2.32 | 4.32/4.39 | 4.03 | 3.88, 3.95 |
| 15°C | 7.32/7.28 | 1.74 | 6.11 | 2.23 | 2.32 | 4.32/4.40 | 4.04 | 3.90, 3.95 |
| 10°C | 7.33/7.28 | 1.73 | 6.12 | 2.21/2.21 | 2.31/2.36 | 4.32/4.41 | 4.04/4.01 | 3.90, 3.95 |
| 5°C[a] | 7.34/7.29 | 1.73 | 6.13 | 2.21/2.21 | 2.31/2.36 | 4.32/4.42 | 4.06/4.01 | 3.91, 3.95 |
| 0°C | 7.34/7.29 | 1.73 | 6.14 | 2.21/2.21 | 2.31/2.36 | 4.33/4.42 | 4.06/4.01 | 3.94, 3.94 |

| | –$COCH_3$ |
|---|---|
| 35°C | 2.03 |
| 25°C | 2.06/1.98 |
| 20°C | 2.07/1.96 |
| 15°C | 2.07/1.96 |
| 10°C | 2.07/1.95 |
| 5°C[a] | 2.08/1.95 |
| 0°C | 2.08/1.95 |

[a] Two chemical shift values separated by a slash indicate the peak splitting.
[b] Measured at 5°C, 800 MHz NMR spectrometer.

interaction between them. The methyl group of $COCH_3$ is close to both moieties of $T_N$ and $_NT$, as well as the base of $_NT$ as shown in Figure 6(A)(2). This structure can be further verified by the same chemical shifts of two $C_5$–$CH_3$'s. This may be caused by the methyl groups (pointed by an arrow) being apart from each other bases and receive the least effect from the rest of $T_NT$ (Fig. 6(A)(2)). The dihedral angle of $\phi_{ON}$ (amide bond ($C_{AC}$–N) along $O_{AC}$–$C_{AC}$–N–$O_{3'}$, see Figure 1) has to be in *trans* domain. This makes $COCH_3$ close to both sugar moieties of $T_N$ and $_NT$, as well as the base of $_NT$ as described previously. Thus, structure derived by chemical shift concurs with that derived by NOE's precisely.

Major form has the same NOE connections at −5°C as well as at high temperatures. Figure 5(c) shows the cross peaks related to the methyl group of –$COCH_3$. For instance, cross peaks *a*, *b*, *c*, *d*, *e*, *f*, and *g* are NOE's of –$COCH_3$ to $C_6$–H ($_NT$), $H_{1'}$ ($T_N$), $H_{3'}$ ($T_N$), $H_{4'}$ ($T_N$), $H_{4'}$ ($_NT$), $H_{5'}$ ($_NT$), and $H_{5''}$ ($_NT$), respectively. The same results were obtained in high temperatures. We thus conclude that the major structure has the same configuration at both −5°C and 55°C (Fig. 6(A)).

### 2.3. The study of minor form of $T_NT$

Likewise, the minor form was studied at −5°C, its NOE pattern was found to be different from that of the major form. As shown in Figure 5(c), the –$COCH_3$ shows no NOE correlations to $C_6$–H ($_NT$), $H_{1'}$ ($T_N$), $H_{4'}$ ($T_N$) (denoted as *x*, *y*, *z* in Figure 5(c)) as the major structure does. This means that the distances between –$COCH_3$ and $C_6$–H ($_NT$), $H_{1'}$ ($T_N$), $H_{4'}$ ($T_N$) may be larger than 5 Å in the minor form. The observed cross peaks between –$COCH_3$ and $H_{3'}$ ($T_N$) as well as –$COCH_3$ and $H_{5'}$/$H_{5''}$ ($_NT$) (Fig. 5(c)) may be caused either by NOE or by chemical exchange of the two structures. The –$COCH_3$ has diminishing NOE to protons of $T_N$ or $_NT$ moieties in minor structure. This result implies that –$COCH_3$ group has swung away from $T_N$ and $_NT$ base and sugar moieties. Therefore, we used long distance constrains (5–20 Å) between –$COCH_3$ and protons of sugars in the proposed structure. Because no clear-cut inter-nucleoside NOE was observed, no constrains were used during MD simulation. Figure 6(B) shows the most plausible result. The –$COCH_3$ swings away, as shown in Figure 6(B) (1) and (2), from both $T_N$ and $_NT$ moieties. The dihedral angle along amide bond and $\phi_{ON}$ along $O_{AC}$–$C_{AC}$–N–$O_{3'}$ was *cis* form in this structure. Two thymine bases are in parallel but separated at a distance from each other.

### 2.4. The structure of 2′-deoxy-D-ribofuranose (sugar)

The structure of sugar in $T_NT$ can be determined by coupling constants of sugar proton resonance.[15] The data at 55°C are listed in Table 2. The values of $J_{H1'-2'}$, $J_{H1'-2''}$, and $J_{H3'-4'}$ are similar to those in TpT.[13] Thus the structures of sugar moieties of $T_N$ and $_NT$ at high temperature are in S-type.[15,16] No accurate coupling constants of either major or minor form were yielded from NMR spectra at low temperatures due to the crowdedness of splitting peaks except the $J_{H1'-2'}$, $J_{H1'-2''}$

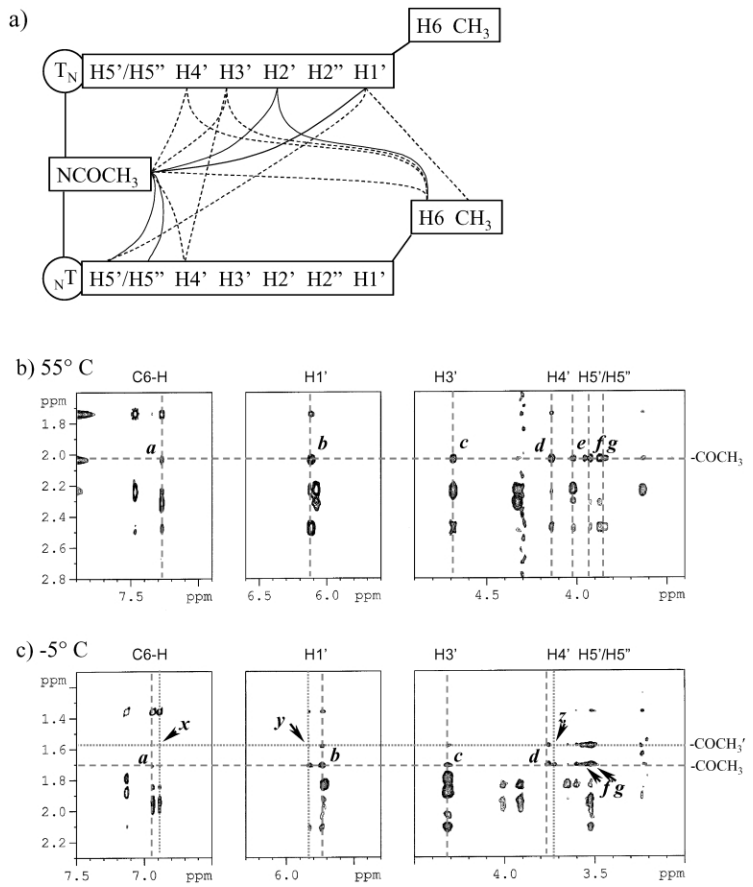


**Figure 5.** (a) The NOE connection map of $T_NT$ in major structure at 55°C. The solid and broken lines represent medium (for distance 3–5 Å) and weak (for distance 4–5.5 Å) NOE, respectively. (b) and (c) The NOE's between $-COCH_3$ and protons of sugar observed at 55 and −5°C, respectively. The broken lines are the chemical shifts of major structure, while the dotted lines are the chemical shifts of minor structure. The $CH_3$ signals of major and minor structures are denoted as $-COCH_3$ and $-COCH_3'$ in (c), respectively.

of major form (data not shown). Their values are the same as those in high temperatures (Table 2). Therefore, the sugar structures of major form may be identical to those at high temperature. On the other hand, the coupling constants in minor form may also be similar to those at high temperature by judging the linewidths. For this reason, it is plausible to speculate that the sugar structures in minor form are also in S-type.

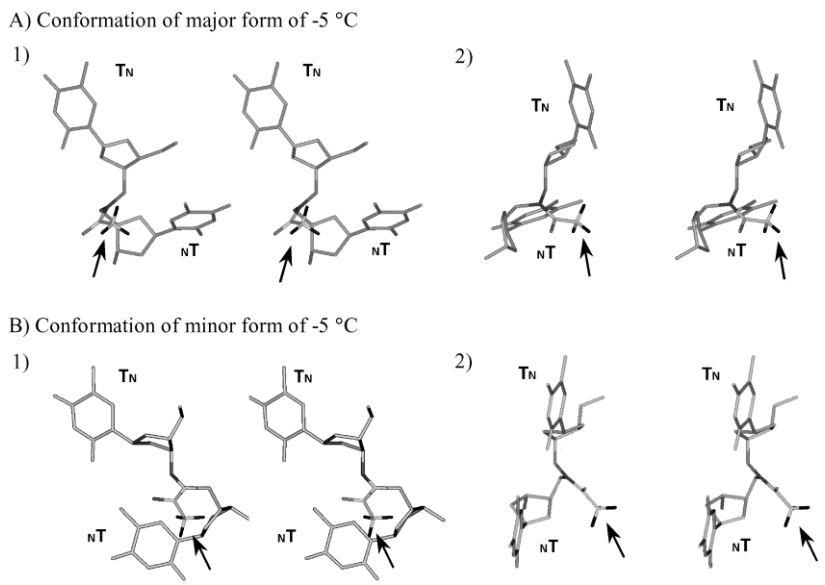


**Figure 6.** The stereo views of major (top) and minor (lower) structures of $T_NT$ are shown in (A) and (B), respectively. Structures (1) and (2) are 90° rotated along $C_{3'}-O_{3'}$ bond to each other. The methyl group is pointed by an arrow for illustration purpose.

**Table 2**. Coupling constants (Hz) of sugar proton resonances

| | $J_{H1'-H2'}$ | $J_{H1'-H2''}$ | $J_{H3'-H2'}$ | $J_{H3'-H2''}$ | $J_{H3'-H4'}$ | $J_{H4'-H5'}$ | $J_{H4'-H5''}$ |
|---|---|---|---|---|---|---|---|
| $T_N$ | 6.14 | 8.19 | 6.14 | 2.30 | 2.3 | 4.35 | 4.35 |
| $_NT$ | 6.66 | 6.66 | 6.14 | 6.14 | 4.10 | 7.42 | 3.58 |

### 2.5. The configuration along the glycosidic bond

2D-NOESY experiments were used to obtain information about the orientation of T base relative to its sugar ring (*syn* or *anti*). The cross peaks between $C_6$–H and $H_{1'}$ of both bases in the major form were observed and they were of medium intensity. Because they were not as strong as the intensity of cross peak between $H_{1'}$ and $H_{2'}$, the glycosidic bond is in *anti*-configuration. Similar intensity was also observed from cross peak between $C_6$–H and $H_{1'}$ in minor form. Thus, the glycosidic bond of minor structure is also in *anti*-configuration.

### 2.6. The comparison of the backbone of the major and minor forms

The primary difference between the major and the minor forms is the bond configuration along the (*N*-acetyl)imino backbone. As shown in Figure 7, the corresponding torsion angles of the two structures are totally different: (1) $\varepsilon'$ torsion angle is located within *trans* domain in the major form but within *gauche* $^-$ domain in the minor; (2) $\phi_{ON}$ torsion angle is located within *gauche* $^+$ domain in the major form but within *gauche* $^-$ domain in the minor form; (3) $\phi_{NC}$ torsion angle is located within *gauche* $^+$ domain in the major form but within *gauche* $^-$ domain in the minor from;

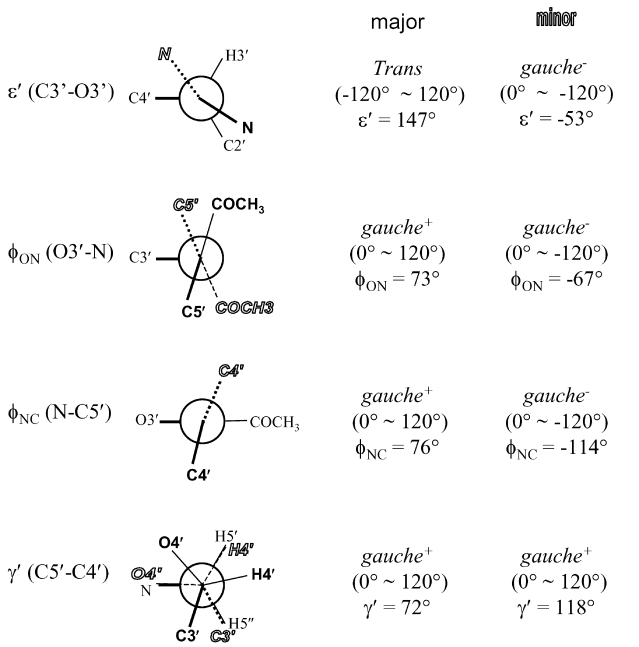


**Figure 7.** The comparison of the backbone between major and minor forms. The bonds' torsion angles are highlighted by thick line for major form, dotted line for minor form. The solid bold Arial-type capital letters are denoted as the atom of major structure. The hollow capital letters are denoted as the atom of minor structure. The regular Time New Roman capital letters are denoted as the overlap atoms of major and minor structures.

(4) $\gamma'$ torsion angles are located within *gauche* $^+$. However, the atoms on the side of $\gamma'$ torsion angle are staggered in the major structure, those of the minor structure are eclipsed. It should be noted that all torsion angles along the backbone in the major structure are in staggered configuration. The repulsion, which can be stabilized by lowering the temperature, between O4′ of $_NT$ and N atom of backbone may result in a structure containing higher potential energy.

## 3. Discussion

### 3.1. The chemical shift differences between major and minor forms

The two T bases are apart from each other in both the major and the minor forms (Fig. 6). Thus, the ring current shielding and de-shielding effect to each other in those bases are negligible. Therefore, each base in $T_NT$ behaves like a monomer in solution. This is why $C_5$–$CH_3$ groups of $T_N$ and $_NT$ and $C_6$–H of $T_N$ of both major and minor forms have nearly identical (within 0.01 ppm) chemical shifts. The $C_6$–H ($_NT$) in minor form shifted 0.05 ppm upfield from that of the major form. This is because it was shielded by the carbonyl group but not by the base. The $C_6$–H of $_NT$ lies on top of the $C_{AC}$=$O_{AC}$ double bond and affected by a shielding effect (Fig. 6(B)).[17] On the contrary, the same proton in major structure locates near the $C_{AC}$ atom (Fig. 6(A)). However, the $C_6$–H shifting to up-field in minor form is minimal due to the poor ring current effect of the carbonyl group.

Similarly, the $-COCH_3$ group of major structure locates on the side of the T base of $_NT$ whereas on the base plane in the minor form (Fig. 6). Therefore, the $CH_3$ in $-NCOCH_3$ has experienced ring current shielding effect in minor form but de-shielding effect in the major form. The splitting is up to 0.08 ppm since the ring current effect is stronger than that in $C_{AC}$=$O_{AC}$ double bond. On the other hand, the sugar protons are closer to the backbone linkage than those on base, although they experienced chemical shift changes from zero (outside protons like $H_{5'}$ and $H_{5''}$) to 0.03–0.04 ppm (protons in medium distance such as $H_{4'}$ and $H_{3'}$) then to 0.08–0.10 ppm of the closest protons ($H_{1'}$, $H_{2'}$, and $H_{2''}$). The results listed in Table 1 were consistent to the structures of major and minor forms. The current structures of major and minor form give a reasonable explanation of chemical shift observation.

### 3.2. Comparison to structure of d-TpT

The structures of thymidine dinucleotide related compounds: pTpT and TpT have been studied by X-ray crystallography[18] and NMR,[19–21] respectively. All these studies reached similar conclusion. Namely, the glysicodic bond of T bases are in *anti* conformation, sugar pucker in S-type. The T bases do not stack well and form an acute angle 38° according to the crystal study. Results from NMR deduce the similar conclusion. However, no two distinctly different structures were found in TpT as observed by NMR. Instead, for both the major and the minor forms in $T_NT$, the two T bases in TpT rotate with respect to each other continuously in the temperature range studied (5–80°C). It

is interesting to note that the $C_6$–H′s of TpT shifted to up field when temperature goes up. The $C_6$–H is sensitive to base stacking. The up field shift suggests that $C_6$–H experiences the shielding effect of T base during the rotation. The faster the rotation exerts the bigger the effect. The structure of T nucleoside in $T_NT$ is similar to that in TpT or pTpT, but the backbone is different in aqueous solution. The backbone O–N(COCH3)–O not only made two T nucleotides spread out but also showed two distinct structures in NMR (400, 500, and 800 MHz) time scale. The free rotation along $\phi_{ON}$ and $\phi_{NC}$ may be hindered by the partial double bond character of the C–N bond as shown in following schematic drawing. The slightly favored major form (60%) may be stabilized by the hydrophobic force to the methyl group toward the T base. However, further verification is needed.

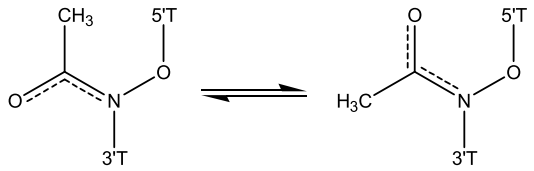


major minor

## 4. Conclusion

$T_NT$ bears an electrically neutral (*N*-acetyl)imino linkage in oligonucleotide backbone and shows a different backbone from that in TpT. The striking result is that $T_NT$ shows two distinct backbone structures in temperature lower than 25°C in observed NMR time scale (400–800 MHz). These two forms are similar in no base stacking, S-type sugar but different along the (*N*-acetyl)imino backbone. In addition, these two structures are not energetically equal. The favored form occupies 60% of the population and the minor one 40%. However, there is a stacking position in $T_NT$ during the inter-conversion between major and minor forms. This will facilitate base pairing with adenine bases in an oligonucleotide of even longer chains. Therefore, $T_NT$ is a potential antibiotics without sacrificing the stability. A long oligonucleotidyl chain containing $T_NT$ fragment will be studied in the future to verify predictions.

## 5. Experimental

The synthesis and purification of $T_NT$ (Fig. 1) were published elsewhere.[9] 2 mg of $T_NT$ was dissolved in 0.5 mL $D_2O$ to make 8 mM in final concentration with 0.1 M NaCl, pH 6.1 without buffer. The $^1H$ NMR data were collected mainly on a Bruker AVANCE-500, and assisted by a Bruker Avance-800 and AM-400 spectrometer. 1D spectra were acquired at −5[†] to 55°C with 5°C interval.

2D COSY and 2D NOESY experiments were performed with 3,592 spectral width, 512 $t_1$-increment at 55, 35, and −5°C, respectively. 32 Scans were accumulated for each fid with 1024 TPPI complex data number. The mixing time of 2D-NOESY was set at 400 and 800 ms, respectively. Fids were apodized with 90°-shifted square sine window function and the processed matrix sizes were 1024×1024 in real point.

The structure was calculated by (1) distance–geometry (DG): Embedding protons within distance constrain ranges to build ca. 30 initial structures. (2) Molecular dynamic simulation (MD): Molecules were energy minimized for 200 steps steepest descents and 200 steps conjugate gradient algorithm. Molecules were furthermore heated to 300 K and run dynamics for 10,000 steps by 10 ps. A distance dependent dielectric constant of 4*r* and p1-4 (1–4 electrostatic interaction) scaling of 1 (means p1–4 is weighed) were used during MD calculation. Finally, molecules were energy minimized again for 2000 steps by using conjugate gradient method. All calculations were performed on Silicon Graphics O2 workstation with DGII and Discover programs utilizing the CVFF force field in Insight II (Accelrys Inc., San Diego, CA, USA).

[†] The probe temperature was measured at −5.3°C by thermocouple in an nmr tube with chloroform. This experiment has been repeated many times and no single case with frozen was seen. The sample may be in supercooling condition.

## Acknowledgements

We are indebted to Dr Detlef Mueller for running the 800 MHz NMR spectra at Bruker Spectrospin at Karlsruhe, Germany. This work is supported by NSC (91 2113 M 001032 to lsk).

## References

1. Vassuer, J.-J.; Debart, F.; Sanghvi, Y. S.; Cook, P. D. *J. Am. Chem. Soc.* **1992**, *114*, 4006–4007.
2. De Mesmaeker, A.; Haner, R.; Martin, P.; Moser, H. E. *Acc. Chem. Res.* **1995**, *28*, 366–374.
3. Swayze, E. E.; Sanghvi, Y. S. *Synlett* **1997**, 859–861.
4. Peterson, M. A.; Nilsson, B. L.; Sarker, S.; Doboszewski, B.; Zhang, W.; Robins, M. J. *J. Org. Chem.* **1999**, *64*, 8183–8192.
5. Li, H.; Miller, M. J. *Tetrahedron Lett.* **2000**, *41*, 4323–4327.
6. Burgess, K.; Gibbs, R. A.; Metzker, M. L.; Raghavachari, R. *J. Chem. Soc., Chem. Commun.* **1994**, 915–916.
7. Witch, E. M.; Cosstick, R. *Tetrahedron Lett.* **1997**, *38*, 6745–6748.
8. Baeschlin, D. K.; Hyrup, B.; Benner, S. A.; Richert, C. *J. Org. Chem.* **1996**, *61*, 7620–7626.
9. Yang, T.-F.; Chien, F.-C.; Chung, F.-Y. *J. Chin. Chem. Soc.* **2001**, *48*, 949–952.
10. Wüthrich, K. *NMR of Proteins and Nucleic Acids*; Wiley: New York, 1986.
11. Gurjar, M. K.; Kunwar, A. C.; Reddy, D. V.; Islam, A.; Lalitha, S. V. S.; Jagannadh, B.; Rama Rao, A. V. *Tetrahedron* **1993**, *49*, 4373–4382.
12. Gabino, J.; Yang, T.-F.; Wright, G. E. *Tetrahedron* **1994**, *50*, 11363–11368.
13. Glemarec, C.; Nyilas, A.; Sund, C.; Chattopadhyaya, J. *J. Biochem. Biophys. Met.* **1990**, *21*, 311–332.
14. Ts'o, P. O. P. *Basic Principles in Nucleic Acid Chemistry*; Academic: New York, 1974; Vol. 2. pp 305–469.

15. Rinkel, L. J.; Alton, C. *J. Biomol. Struct. Dynam.* **1987**, *4*, 621–649.
16. Cheng, D. M.; Kan, L.-S.; Leutzinger, E. E.; Jayaraman, K.; Miller, P. S.; Ts'o, P. O. P. *Biochemistry* **1982**, *21*, 621–630.
17. Bible, Jr.R. H. *Interpretation of NMR Spectra: An Empirical Approach*; Plenum: New York, 1965; pp 7–48.
18. Camerman, N.; Fawcett, J. K.; Camerman, A. *Science* **1973**, *82*, 1142–1143.
19. Woods, D. J.; Ogilvie, K. K.; Hruska, F. E. *Can. J. Chem.* **1975**, *53*, 2781–2790.
20. Rycyna, R. E.; Alderfer, J. A. *Nucl. Acids Res.* **1985**, *13*, 5949–5963.
21. Rycyna, R. E.; Wallance, J. C.; Sharma, M.; Alderfer, J. A. *Biochemistry* **1988**, *27*, 3152–3163.